



# Structural and Electrical Properties of $\text{Co}_x\text{Mn}_{3-x}\text{O}_4$ Ceramics for Negative Temperature Coefficient Thermistors

Kyeong-Min Kim, Sung-Gap Lee<sup>†</sup>, and Min-Su Kwon

Department Materials Engineering and Convergence Technology, Engineering Research Institute,  
Gyeongsang National University, Jinju 52828, Korea

Received June 9, 2017; Accepted July 21, 2017

$\text{Co}_x\text{Mn}_{3-x}\text{O}_4$  ( $1.48 \leq x \leq 1.63$ ) ceramics were fabricated using the solid-state reaction method. Structural and electrical properties of specimens based on the composition ratio of Co were observed in order to investigate their applicability in NTC thermistors. All specimens showed a single spinel phase with a homogeneous tetragonal structure. The  $\text{Co}_{1.57}\text{Mn}_{1.43}\text{O}_4$  specimen showed a maximum average grain size of approximately 6.47  $\mu\text{m}$ . In all specimens, TCR properties displayed excellent characteristics of over  $-4.2\%/^\circ\text{C}$ . The resistivity at 298 K and B-value of the  $\text{Co}_{1.57}\text{Mn}_{1.43}\text{O}_4$  specimen were approximately 418  $\Omega\text{-cm}$  and 4300, respectively.

**Keywords :** Infrared detector,  $\text{Ni}_{0.79}\text{Co}_{0.15-x}\text{Cu}_x\text{Mn}_{2.06}\text{O}_4$ , Responsivity, Solid-state reaction method, Thick film

## 1. INTRODUCTION

The transition metal manganite  $\text{M}_x\text{Mn}_{3-x}\text{O}_4$  has an  $\text{AB}_2\text{O}_4$  spinel structure in which a  $\text{M}^{2+}$  ion is present in the tetrahedral A-site and a  $\text{Mn}^{3+}$  ion is distributed in the octahedral B-site, and has been studied for a long time as an NTCR (negative temperature coefficient of resistance) thermistor material where resistance changes with temperature [1]. Recently, applications of these passive components have expanded to various fields such as temperature measurement and circuit compensation devices in the aerospace industry, in addition to the automobile and medical fields. The electrical conduction phenomenon of transition metal manganite ceramics is attributed to the hopping conduction mechanism caused by an electron jump between  $\text{Mn}^{3+}$  and  $\text{Mn}^{4+}$  ions located at the octahedral sites. As some of the  $\text{M}^{2+}$  ions are located in octahedral sites, some of the  $\text{Mn}^{3+}$  ions are ionized to  $\text{Mn}^{4+}$  to maintain electrical neutrality [2]. Generally, electrical resistivity strongly depends on the composition and structural characteristics of such oxides, because the electrical

characteristics are influenced by the distribution of the cations at the two sites, tetrahedral and octahedral, of the spinel structure. In this study, cobalt manganite  $\text{Co}_x\text{Mn}_{3-x}\text{O}_4$  ceramics were fabricated in order to improve the resistivity and temperature-sensitive resistance characteristics at approximately room temperature. The structural and electrical properties were measured to investigate the possibility of their application in NTC thermistor devices.

## 2. EXPERIMENTS

In this study,  $\text{Co}_x\text{Mn}_{3-x}\text{O}_4$  ( $1.48 \leq x \leq 1.63$ ) ceramics were fabricated by the solid-state reaction method using high-purity  $\text{Co}_3\text{O}_4$  (Aldrich, 99%) and  $\text{Mn}_2\text{O}_3$  (Aldrich, 99%) powders as starting materials. Each sample was weighed according to the composition formula, and then mixed and ground with ethyl alcohol as the dispersion medium for 24 hours using zirconia balls. The mixed powders were calcined at 900  $^\circ\text{C}$  for 2 hours and an organic binder (3 wt%) was added. The specimens were sintered at 1,200  $^\circ\text{C}$  for 12 hours, and slowly cooled to 800  $^\circ\text{C}$ , held for 10 min, and then quenched to room temperature. The structural properties based on the Cu ion composition ratio were analyzed by X-ray diffraction (XRD) and field-emission scanning electron microscopy (FE-SEM). To measure the electrical properties, Ag electrodes were attached to the surface of the thick films by the screen-printing method. Electrical resistance was measured with an electrometer (Keithley 6517A, USA) from  $-10\text{ }^\circ\text{C}$  to 60  $^\circ\text{C}$ .

<sup>†</sup> Author to whom all correspondence should be addressed:  
E-mail: [lsgap@gnu.ac.kr](mailto:lsgap@gnu.ac.kr)

Copyright ©2017 KIEEME. All rights reserved.

This is an open-access article distributed under the terms of the Creative Commons Attribution Non-Commercial License (<http://creativecommons.org/licenses/by-nc/3.0>) which permits unrestricted noncommercial use, distribution, and reproduction in any medium, provided the original work is properly cited.

### 3. RESULTS AND DISCUSSION

Figure 1 shows the DTA-TG thermal analysis of  $\text{Co}_{1.60}\text{Mn}_{1.40}\text{O}_4$  powder. An exothermic peak accompanied by a mass reduction was observed at approximately  $200^\circ\text{C}$ , which is attributed to the combustion of water and organic materials. The mass changes in the range of  $400\text{--}900^\circ\text{C}$  are due to the oxidation and reduction of  $\text{Mn}^{3+}$  ions into  $\text{Mn}^{2+}$  and  $\text{Mn}^{4+}$  and/or  $\text{Co}^{2+}$  into  $\text{Co}^{III}$  [3,4]. It is considered that the small exothermic peak accompanied with the mass loss at approximately  $1,000^\circ\text{C}$  is due to the formation of the stoichiometric spinel phase,  $\text{Co}_x\text{Mn}_{3-x}\text{O}_4$ .

Figure 2 shows the X-ray diffraction patterns of  $\text{Co}_x\text{Mn}_{3-x}\text{O}_4$  specimens. All specimens displayed a single phase tetragonal spinel structure and changes in the XRD patterns based on Co composition were not observed.

Figure 3 shows the surface microstructure of  $\text{Co}_x\text{Mn}_{3-x}\text{O}_4$  specimens as a function of Co composition. All specimens displayed a relatively dense microstructure, and dependence of average grain size on Co composition ratio was not observed. The  $\text{Co}_{1.57}\text{Mn}_{1.43}\text{O}_4$  specimen showed a maximum average grain size of approximately  $6.47\ \mu\text{m}$ .

Figure 4 shows the electrical resistance based on Co composition and the temperature of  $\text{Co}_x\text{Mn}_{3-x}\text{O}_4$  specimens. All specimens displayed typical NTCR characteristics, where resistance exponentially decreases with an increase in temperature, and exhibited excellent NTCR properties of greater than  $-4.2\%/^\circ\text{C}$ .

Figure 5 shows the resistivity at  $298\text{K}$  of  $\text{Co}_x\text{Mn}_{3-x}\text{O}_4$  specimens. Resistivity was a constant value of approximately  $450\ \Omega\text{-cm}$  for Co composition ratios of  $1.48$  to  $1.57$ , but increased when the Co

composition ratio was  $1.60$  or greater. In general, for  $1 < x < 3$ ,  $\text{Co}^{2+}$  ions are distributed in all tetrahedral sites, and some  $\text{Co}^{2+}$  ions are substituted with  $\text{Mn}^{3+}$  ions at octahedral sites. That is,  $2\text{Mn}^{3+}_{\text{oc}} \rightarrow \text{Co}^{2+}_{\text{oc}} + \text{Mn}^{4+}_{\text{oc}}$  with the creation of  $\text{Mn}^{3+}\text{-Mn}^{4+}$  pairs. In addition,  $\text{Co}^{2+}\text{-Co}^{III}$  pairs (with a low spin state of  $t_{2g}^6e_g$ ) [5,6] are formed on the Co-rich

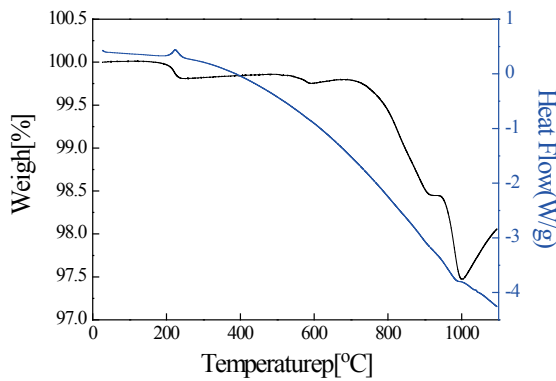


Fig. 1. DTA-TG curves for  $\text{Co}_{1.60}\text{Mn}_{1.40}\text{O}_4$  ceramics.

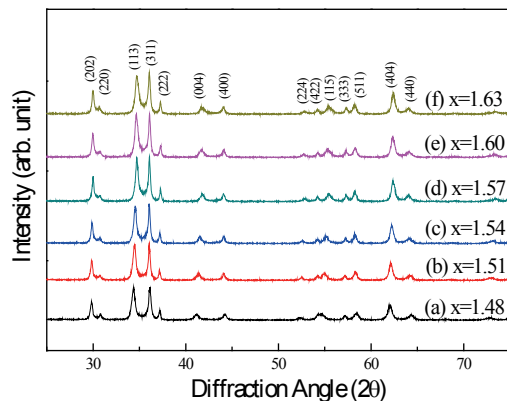


Fig. 2. X-ray diffraction patterns of  $\text{Co}_x\text{Mn}_{3-x}\text{O}_4$  ceramics; (a)  $x=1.48$ , (b)  $x=1.51$ , (c)  $x=1.54$ , (d)  $x=1.57$ , (e)  $x=1.60$ , and (f)  $x=1.63$ .

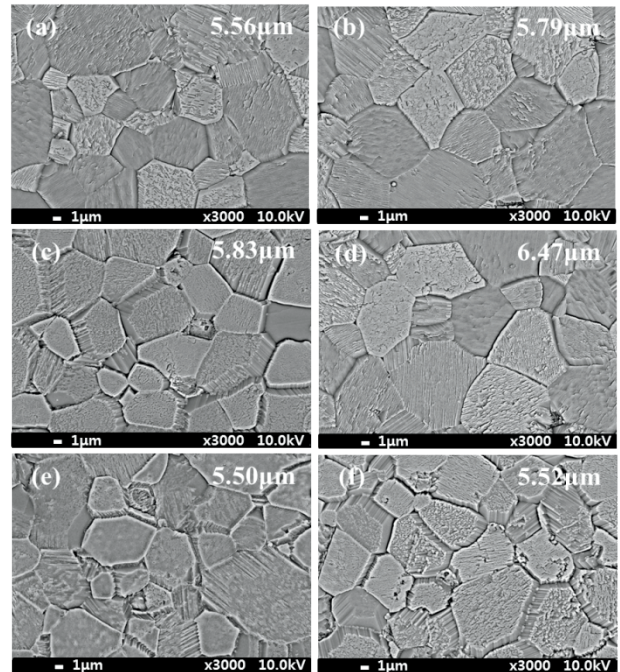


Fig. 3. FE-SEM surface image of  $\text{Co}_x\text{Mn}_{3-x}\text{O}_4$  ceramics. (a)  $x=1.48$ , (b)  $x=1.51$ , (c)  $x=1.54$ , (d)  $x=1.57$ , (e)  $x=1.60$ , and (f)  $x=1.63$ .

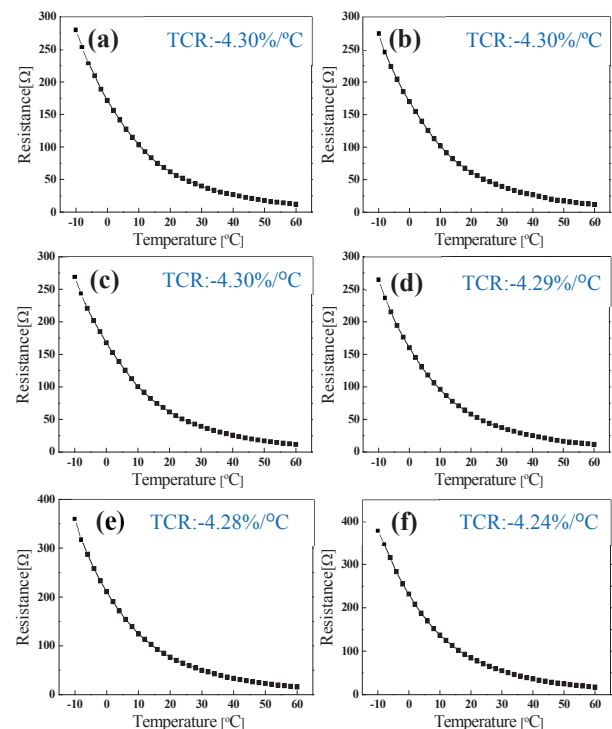


Fig. 4. Temperature-Resistance properties of  $\text{Co}_x\text{Mn}_{3-x}\text{O}_4$  ceramics. (a)  $x=1.48$ , (b)  $x=1.51$ , (c)  $x=1.54$ , (d)  $x=1.57$ , (e)  $x=1.60$ , and (f)  $x=1.63$ .

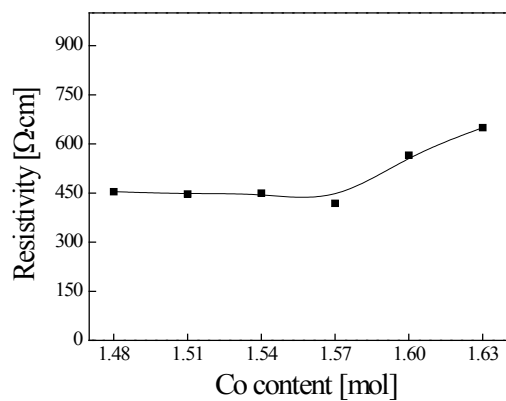


Fig. 5. Resistivity (at R.T.) of  $\text{Co}_x\text{Mn}_{3-x}\text{O}_4$  ceramics with varying Co content.

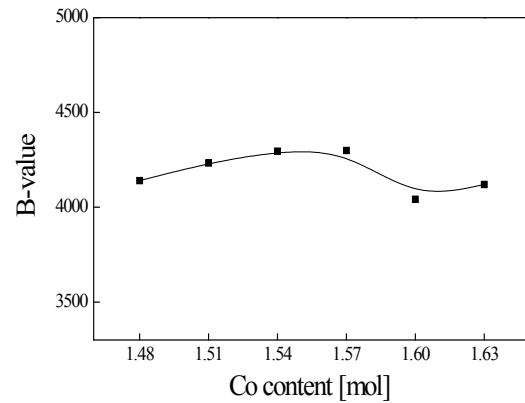


Fig. 7. B-value of  $\text{Co}_x\text{Mn}_{3-x}\text{O}_4$  ceramics with varying Co content.

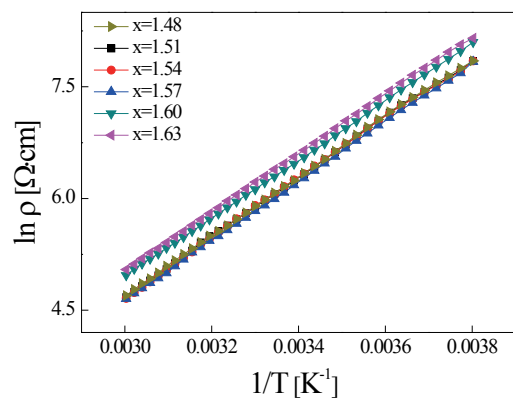


Fig. 6.  $\ln \rho$  vs  $1/T$  plot of  $\text{Co}_x\text{Mn}_{3-x}\text{O}_4$  ceramics with varying Co content.

phase and act as donors or acceptors. These manganese and cobalt pairs contribute to hopping conduction and the resistivity characteristics are reduced [7,8]. However, when the composition ratio of Co increases above the critical value, the concentration of  $\text{Co}^{\text{III}}$  ions in octahedral sites gradually increases, while the concentration of  $\text{Co}^{2+}$  ions decreases. Also, as the concentration of  $\text{Mn}^{3+}$  ions decreases, conductivity decreases due to a decrease in  $\text{Co}^{2+}$ - $\text{Co}^{\text{III}}$  and  $\text{Mn}^{3+}$ - $\text{Mn}^{4+}$  pairs [9]. In this study, the threshold value of the Co composition that increases resistivity was  $x=1.60$  and depends on the composition ratio, sintering temperature and time, and quenching conditions.

Figure 6 shows the  $\ln \rho$  vs  $1/T$  relationship for  $\text{Co}_x\text{Mn}_{3-x}\text{O}_4$  specimens. Generally, the conductivity of transition metal oxides like spinel manganites  $\text{Mn}_{3-x}\text{M}_x\text{O}_4$  ( $\text{M}=\text{Ni}, \text{Cu}, \text{Co}\dots$ ), is due to the presence of donor/acceptor  $\text{M}^{n+}/\text{M}^{(n+1)+}$  couples in the octahedral sites (such as  $\text{Mn}^{3+}/\text{Mn}^{4+}$ ) that contribute to an electronic exchange via a hopping mechanism according to Verwey's law [10,11]. The  $\text{Co}_x\text{Mn}_{3-x}\text{O}_4$  specimens show a linear relationship between  $\ln \rho$  and  $1/T$  over the measured temperature range, thus indicating the typical NTC thermistor characteristics described by the Nernst-Einstein relation [12]. This is due to the fact that both  $\text{Mn}^{3+}/\text{Mn}^{4+}$  and  $\text{Co}^{2+}/\text{Co}^{\text{III}}$  pairs on the octahedral sites act as hopping ions.

Figure 7 shows the B-value of  $\text{Co}_x\text{Mn}_{3-x}\text{O}_4$  specimens. The thermal sensitivity of a material's resistance, usually noted as B, is directly related to the activation energy  $E_a$  through the relationship  $B=E_a/k$ , where  $k$  is Boltzmann's constant. B-value increased with an increase in the composition ratio of Co from  $x=1.48$  to  $1.57$ ; however, it decreased slightly for compositions of  $x \geq 1.60$ . For  $1.48 \leq x \leq 1.57$ , as discussed in Fig. 5, with increase in the composition ratio of Co with its small ionic radius,  $\text{Co}^{2+}/\text{Co}^{\text{III}}$  pairs increased and the distance

between metal ions at octahedral sites decreased [13]. For  $x \geq 1.60$ ,  $\text{Co}^{2+}$  ions decreased and  $\text{Co}^{\text{III}}$  concentration increased in order to minimize tetragonal distortion in the lattice structure.

## 4. CONCLUSIONS

In this study, the structural and electrical properties of cobalt manganite system ceramics were investigated for application in NTC thermistors. All specimens displayed the single phase tetragonal spinel structure and dependence of average grain size on the Co composition ratio was not observed.  $\text{Co}_x\text{Mn}_{3-x}\text{O}_4$  specimens exhibited a linear relationship between resistivity and temperature, thus indicating the typical NTC thermistor characteristics. This is due to the fact that both  $\text{Mn}^{3+}/\text{Mn}^{4+}$  and  $\text{Co}^{2+}/\text{Co}^{\text{III}}$  pairs at octahedral sites act as hopping ions. In general, as the composition ratio of Co increases, the concentration of  $\text{Co}^{2+}$  ions located in octahedral sites increases.  $\text{Mn}^{3+}/\text{Mn}^{4+}$  and  $\text{Co}^{2+}/\text{Co}^{\text{III}}$  pairs are formed to maintain electrical neutrality. However, when the composition ratio of Co increases above the critical value,  $\text{Co}^{2+}$  ions decrease and  $\text{Co}^{\text{III}}$  concentration increase in order to minimize tetragonal distortion in the unit cell. In this study, this value was  $x=1.60$ , and it depends on the composition ratio, sintering temperature and time, and quenching conditions.

## ACKNOWLEDGMENT

This work was supported by the Industrial Strategic Technology Development Program (No. 10045177, Development of Resistive Ceramic Thin Film using Solution Process and Low Temperature Thin Film Vacuum Getter).

## REFERENCES

- [1] K. E. Sickafus, J. M. Wills, and N. W. Grimes, *J. Am. Ceram. Soc.*, **82**, 3279 (1999). [DOI: <https://doi.org/10.1111/j.1151-2916.1999.tb02241.x>]
- [2] X. X. Tang, A. Manthiram, and J. B. Goodenough, *J. Less-Common Met.*, **156**, 357 (1989). [DOI: [https://doi.org/10.1016/0022-5088\(89\)90431-1](https://doi.org/10.1016/0022-5088(89)90431-1)]
- [3] K. Park and J. K. Lee, *Scripta Mater.*, **57**, 329 (2007). [DOI: <https://doi.org/10.1016/j.scriptamat.2007.04.026>]
- [4] D. L. Fang, Z. B. Wang, P. H. Yang, W. Liu, C. S. Chen, and A.J.A. Winnubst, *J. Am. Ceram. Soc.*, **89**, 230 (2006). [DOI: <https://doi.org/10.1111/j.1551-2916.2005.00666.x>]
- [5] B. Boucher, R. Buhl, R. D. Bella, and M. Perrin, *J. Phys. France*, **31**, 113 (1970). [DOI: <https://doi.org/10.1051/jphys:01970003101011300>]

- [6] D. G. Wickham and W. J. Croft, *J. Phys. Chem. Solids*, **7**, 351 (1958). [DOI: [https://doi.org/10.1016/0022-3697\(58\)90285-3](https://doi.org/10.1016/0022-3697(58)90285-3)]
- [7] B. Gillot, R. Legros, R. Metz, and A. Rousset, *Solid State Ionics*, **51**, 7 (1992). [DOI: [https://doi.org/10.1016/0167-2738\(92\)90337-O](https://doi.org/10.1016/0167-2738(92)90337-O)]
- [8] H. Bordeneuve, A. Rousset, C. Tenailleau, and S. Guillemet-Fritsch, *J. Therm. Anal. Calorim.*, **101**, 137 (2010) [DOI: <https://link.springer.com/article/10.1007/s10973-009-0557-7>]
- [9] H. Bordeneuve, C. Tenailleau, S. Guillemet-Fritsch, R. Smith, E. Suard, and A. Rousset, *Solid State Sci.*, **12**, 379 (2010). [DOI: <https://doi.org/10.1016/j.solidstatesciences.2009.11.018>]
- [10] A. Rousset, C. Tenailleau, P. Dufour, H. Bordenenve, I. Pasquet, S. Guillemet-Fritsch, V. Poulain, and S. Schuurman, *Int. J. Appl. Ceram. Technol.*, **10**, 175 (2013). [DOI: <https://doi.org/10.1111/j.1744-7402.2011.02723.x>]
- [11] G. P. Vasil'ev, L. A. Pakhomov, and L. A. Ryabova, *Thin Solid Films*, **66**, 119 (1980). [DOI: [https://doi.org/10.1016/0040-6090\(80\)90213-8](https://doi.org/10.1016/0040-6090(80)90213-8)]
- [12] S. E. Dorris and T. O. Mason, *J. Am. Ceram. Soc.*, **71**, 379 (1988). [DOI: <https://doi.org/10.1111/j.1151-2916.1988.tb05057.x>]
- [13] R. D. Shannon, *Acta Cryst.*, **A32**, 751 (1976). [DOI: <https://doi.org/10.1107/S0567739476001551>]